Table 1 Yield of C_4–C_7 hydrocarbons from microbial degradation of terpenoids

Mixed culture	Substrate*	Products	Yield† (μg per litre medium)
Metal cans			
Anaerobes	Farnesol	Isopentane	3
		3-Methylpentane	1.5 ± 0.3‡
Anaerobes	β-Carotene	2-Methylpentane	19
		3-Methylpentane	16 ± 2.5‡
		Toluene	35
Serum bottles			
Anaerobes	Farnesol	1-Butene	12
		3-Methylpentene	11
Anaerobes	β-Carotene	Methylbutene	14
Anaerobes	α-2-Pinene	Methylbutene	15
Aerobes (7 days) / Anaerobes (8 days)	Farnesol	1-Butene	141
		2-Hexene	9
Aerobes (7 days) / Anaerobes (8 days)	β-Carotene	1-Hexene	30
Aerobes (7 days) / Anaerobes (8 days)	α-2-Pinene	Methylpentene	17
		2,2-Dimethylbutane	21

* About 0.5–1.5 mg of substrate per ml of medium.
† Detection limit 0.003 μg per litre medium.
‡ Standard deviation from duplicate cultures.

with substrate but no bacteria. Small amounts of methane, ethane, propane and butanes were found in some of the samples, but these were also in blanks that did not contain the terpenoids, so their presence was not considered a result of terpenoid degradation. Also, the samples run in the serum bottles with anaerobic bacteria, but no terpenoids, yielded 50 μg per litre of dimethylsulphide and 25 μg per litre of CS_2 (detected by gas chromatography). When farnesol was added, these yields increased up to 60 μg and 200 μg per litre, respectively.

The most significant conclusion is that the anaerobic degradation process formed only a few specific hydrocarbons from each terpenoid. Only alkanes and toluene were formed in the metal cans, whereas alkenes were the main products in the glass serum bottles. The kinetics of alkene formation by the anaerobes is possibly faster than that of alkane formation, but is inhibited by the metal in the can. The formation of branched pentanes from either farnesol or β-carotene is conceivable through the breaking of a carbon–carbon bond in the beta position to the double bonds. It is more difficult to understand the formation of the toluene although methylcyclohexene might be a reasonable precursor[4]. β-Carotene will aromatize to form toluene when heated for 2 weeks at 119 °C (ref. 8). However, when heated at 90 °C for 15 min in the conditions of our experiments, no toluene was found within our detection limit (0.003 μg per litre medium). The high yield of toluene in Table 1 only resulted when anaerobes were present in the can. The reason for formation of toluene in the cans but not in the bottles is unclear, but may be due to some effect of the metal in the can. Controls showing no toluene production were: (1) blanks having all substrates including carotene but no bacteria; and (2) bacteria with all carbon sources except carotene. Thus, toluene production due to a metal-catalysed chemical reaction has been ruled out. We did not do aerobic experiments with the metal cans so we cannot conclude that toluene forms exclusively in anaerobic environments.

The anaerobic culturing in the serum bottles yielded mainly branched alkenes. The experiments with aerobes followed by anaerobes yielded mainly straight-chain alkenes and one gem-dimethyl alkane, 2,2-dimethylbutane. The formation of this compound from α-2-pinene could result from breaking off the 4-carbon ring with the quaternary carbon atom in α-pinene.

The results of these preliminary microbial degradation experiments fit surprisingly well with our studies of hydrocarbon distributions in marine sediments. In the strongly reducing environment of Walvis Bay, we found that toluene constituted 70% of the C_4–C_7 hydrocarbons in the surface sediments[4]. The present laboratory experiments support the concept that toluene can be an anaerobic degradation product, and show that the gem-dimethyl alkanes, such as neopentane and 2,2-dimethylbutane dominate in sediments where the overlying waters (and topmost sediments) are oxidizing with deeper sediments reducing (Arabian Sea)[3]. These same environments also produced a diverse assemblage of alkenes, including straight-chain pentenes and hexenes. Such compounds seemed to arise from a combination of both aerobic and anaerobic microbial degradation of organic substrates, possibly together with low-temperature chemical reactions. Whelan *et al.*[4] have discussed in detail possible chemical reactions leading to the C_4–C_7 hydrocarbons, such as alcohol dehydration and allylic free radical cleavage. It has also been pointed out that bacterial reworking of algae forms an amorphous biomass high in bacterial bodies that is more readily converted to hydrocarbons in the C_{15+} range[9]. However, we found no references to C_4–C_7 hydrocarbon formation by bacterial reworking.

We are not arguing that these products represent major metabolic paths in the organism. The trace amounts of substrate transformed suggest that these paths probably represent reactions which are incidental to the bacteria. However, the small (p.p.m.–p.p.b.) levels of compounds found in these experiments and in our Recent sediment analyses are comparable so that these microbial processes may explain one source of the compounds in Recent sediments. This is a valuable finding because the presence of a particular set of these molecules in more deeply buried cold sediments may provide information about the nature of the sediment–water interface (oxic or anoxic) when the sediment was buried in past geological time.

This work was supported by the Oceanography Section of the NSF grant OCE 79–19861. We thank Craig Taylor for critical evaluation, and Elizabeth McKenna and Marcia Pratt for culturing aerobes and analysing headspaces gases. WHOI No. 4571.

Received 14 July; accepted 14 October 1980.

1. Hunt, J. M. *Nature* **245**, 411 (1975).
2. Whelan, J. K. *Init. Rep. DSDP* **47a**, 531 (1979).
3. Hunt, J. M. & Whelan, J. K. *Org. Geochem.* **1**, 219 (1979).
4. Whelan, J. K., Hunt, J. M. & Berman, J. *Geochim. cosmochim. Acta* (in the press).
5. Ferry, J. G. & Wolfe, R. S. *Microbiology* **107**, 33 (1976).
6. Lyman, J. & Fleming, R. H. *J. Mar. Res.* **3**, 134 (1940).
7. Willingham, C. A. & Oppenheimer, C. H. *J. Bact.* **88**, 541 (1964).
8. Day, W. C. & Erdman, J. G. *Science* **141**, 808 (1963).
9. Lijmbach, G. M. G. *Proc. 9th World Petroleum Congr.* **2**, 357–369 (1975).

The principal eyes of a jumping spider have a telephoto component

David S. Williams & Peter McIntyre

Department of Neurobiology, Research School of Biological Sciences, Australian National University, Canberra, Australia

Jumping spiders are a cosmopolitan family (Salticidae) of predators that can make visual discrimination between prey and mates[1,2]. This task is mediated through the anterior median eyes, described by Land[3] as consisting of a corneal lens and a motile retina that comprises four layers of receptors embedded in a matrix. The retinal matrix contains a pit distal to the receptors and symmetrically centred on-axis. We have now found that in *Portia fimbriata* (Doleschall) and some other species, this pit has a refracting interface that increases the focal length of the eye beyond its axial length, thereby magnifying the retinal image and increasing visual resolving power above that possible with only a corneal lens. The most effective part of the conical pit is its rounded apex, which augments the corneal lens to provide a telephoto system that increases the overall focal length by about 1½ times. This mechanism is of particular value to small spiders like *P. fimbriata*, for the possible axial length of their eyes is constrained by the small size of their prosomae (Fig. 1).

0028–0836/80/500578—03$01.00

The inside of the pit of the anterior median eye of *P. fimbriata* is structureless and must have a refractive index (n) close to that of saline, about 1.336 (Fig. 2). In glutaraldehyde-fixed material, cut while frozen, the matrix behind the pit was found by interferometry to have a uniform n, a value of ~1.40 being obtained from unfixed material. The rounded apex of the pit is about 20 μm in diameter; the most central region is approximately spherical, with radius of curvature −5 μm, and thus acts as the diverging lens of the telephoto system (Fig. 3), with power $(1.40-1.336)/(-5\times10^{-6}) = -12{,}800$ dioptres. In longitudinal profile, the rounded region is less curved beyond about 4 μm from the axis and merges into straight sides (Fig. 2). Such an aspherical surface may well give a better image over a wider aperture than a spherical one. The curvature of the pit varies greatly among the different species of salticids and in some cases is so slight that the pit will have negligible power.

From a corneal lens (diameter 810 μm) of *P. fimbriata*, dissected out and hung from a drop of saline ($n = 1.336$) to simulate *in situ* conditions[4,5], a front focal length of −1,273 μm, that is, a power of +786 dioptres, was measured (in green light, as was used for the measurements of n). The second principal plane of the corneal lens was found nearly to coincide with the front surface of the lens, indicating that the air/cornea interface provides most of the refracting power. The remaining parameter necessary for determination of the optical properties of the telephoto system is the distance, d, between the corneal lens (more precisely, its second principal plane) and the pit. d was deduced from ophthalmoscopy, using an apparatus similar to that devised by Land[3,6]. By finding the position in space of the image of a recognizable part of the retina (in this case the virtual image of parts of the receptor cells in the characteristically organized fourth receptor layer, which on-axis lies 25 μm behind the pit), d can be calculated from standard thick-lens formulae[7]. (Ideally the properties of the complete dioptric system could be determined directly from the magnification of the ophthalmoscopical image, but this was prevented by uncertainty about exactly which parts of the receptor cells in layer 4 provide the image.) The value determined for d (=1,664 μm) is to be compared with the focal length in image space of the corneal lens ($1{,}273\times1.336 = 1{,}701$ μm). To achieve a reasonable magnification without unduly increasing image distance, the pit must be a short distance inside the focal point of the corneal lens. This condition seems to be satisfied.

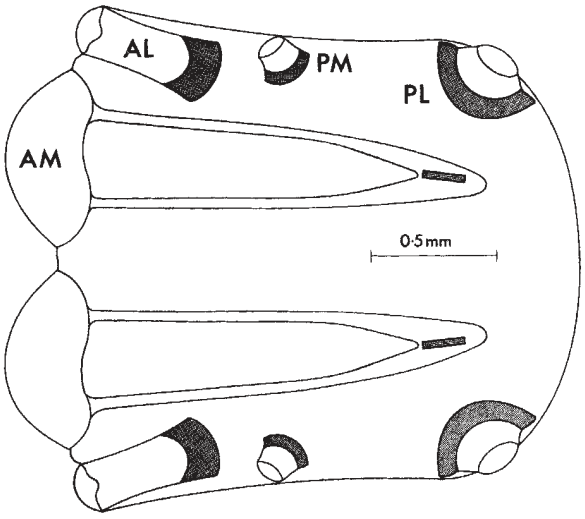

Fig. 1 Diagrammatic horizontal section of the dorsal anterior part of the prosoma of *P. fimbriata*, showing the positions of the anterior (A) and posterior (P) median (M) and lateral (L) eyes. This eye-bearing portion of the prosoma projects dorsally. In the dorso-ventral plane, the posterior eyes lie just above the anterior median retinae.

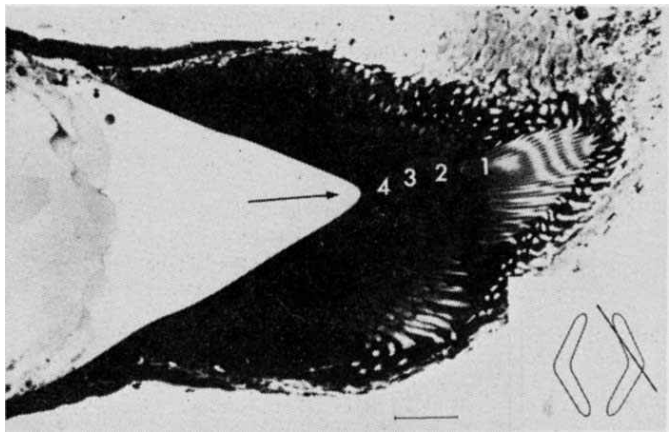

Fig. 2 Longitudinal section of an anterior median retina in *P. fimbriata* including part of one arm of its 'boomerang' structure. The material was fixed in glutaraldehyde and OsO_4, embedded in Araldite and stained with toluidine blue. Scale bar, 50 μm. The interior of the pit (arrow) is structureless (the glass cells visible on the left side of the figure do not extend into the pit), but the surrounding retinal matrix has stained densely and homogeneously. Receptor layers are numbered. Horizontally, across the narrow centre of the retina, the distal ends of the layer 1 receptors are arranged as a staircase, such that on the lateral side of the retina they are 25 μm more distal than on the medial. The overall radius of curvature of the retina in a dorso-ventral plane is far smaller than would be expected if the receptors were organized around the corneal lens. This indicates further that the retina is organized according to the combined properties of the corneal lens and the pit. Inset: Diagram outlining the two anterior median retinae in transverse section at the level of layer 1. The line indicates the plane of the longitudinal section.

Using the above parameters, the position of focus, F', of the telephoto system for an object at infinity is 59 μm behind the pit, corresponding to the distal on-axis region of the second receptor layer, and the magnification achieved by the pit lens is 1.54 (see Fig. 3). The following supports this finding. Comparative ultrastructural studies of salticid principal retinae[8] show that (1) layer 1 receptors in the central region form a high-resolution mosaic whose rhabdom organization implies that the individual rhabdoms are light guides; (2) layer 2 receptors form a coarse central mosaic with probable optical coupling between receptors. In *Plexippus*, recordings from dye-injected cells have identified both layers 1 and 2 as green receptors with peak responses at ~520 nm (ref. 9). Cells peaking in the green have also been found previously[10]; discrepancies between these results and other published data[11] will be discussed elsewhere[9]. Some salticids, including *P. fimbriata*, seem to discriminate between conspecifics and prey at distances of 15–20 cm (refs 12, 13); *Trite planiceps* Simon, a salticid that we find has a significant pit, but lower overall image magnification than *P. fimbriata*, is known to make discriminations at distances of 20 cm (ref. 12). Thus, a 'best solution' for the dioptric system must provide focused images of objects, ~20 cm in front of the spider, at the tips of the rhabdoms of layer 1, when $\lambda = 520$ nm. For F' near the distal ends of the layer 2 receptors, the distal ends of those of layer 1 (Fig. 2) receive best images from objects 15–29 cm in front of the spider and have a total depth of field of 9 cm to ∞. The depth of field is estimated by compounding the horizontal 'staircase' tiering of the distal ends of layer 1 receptors (which gives the 15–29-cm range) with the depth of focus due to diffraction at the aperture of the eye[7] (see below).

The retina of an anterior median eye is boomerang-shaped (Fig. 2), measuring only 250 μm dorso-ventrally and 25 μm wide—a size reduction necessary to accommodate the eye's long axis[3] (Fig. 1). At the level of layer 1, the receptors in the centre of

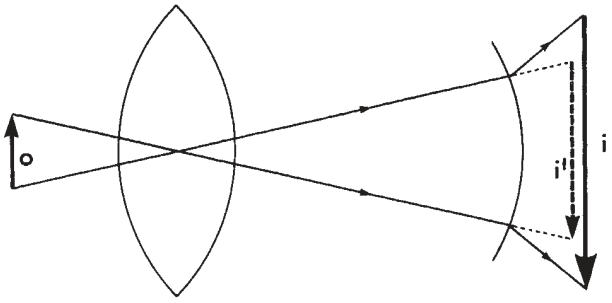

Fig. 3 General schematic illustration of the enlargement of an image by the diverging back element of a telephoto system. o, object; i, image; i', image in absence of diverging surface. The magnification, m, effected by the pit lens in *P. fimbriata* is given by[7]

$$m = \frac{\text{size of i}}{\text{size of i'}} = P_L/P_T = \left[1 + \frac{P_P(1-\bar{d}P_L)}{P_L}\right]^{-1}$$

where P_T is the power of the telephoto lens system, and P_L, P_P the powers of its components, the converging corneal lens and the diverging pit lens respectively. $\bar{d} = d/1.336$, with d as defined in the text. This magnification requires an increase in the axial length of the eye of only 22 μm.

the retina have oval transverse profiles (minimum size 0.8 μm × 1.5 μm) and form an hexagonal array with a minimum receptor-row spacing of 1.4 μm (ref. 8), corresponding to a visual angle of 2.4 arc min. (This corresponds to a distance of 0.12 mm at 20 cm in front of the spider.) The resolving ability of a receptor mosaic depends on the angular subtense between neighbouring receptors, that is, on the receptor spacing and focal length of the eye. The receptor spacing at the centre of layer 1 is near the limit imposed by the wave nature of light, because optical crosstalk[14] between the 80–100-μm long rhabdoms would probably be excessive were they much closer together. Therefore, the only way to enhance the anatomical resolving power of the eye is to increase its focal length. Image magnification by the pit achieves this, albeit at the cost of narrowing the field of view of the central retina. About 100 receptors in the centre of layer 1 lie behind the curved region of the pit in a circle of diameter 21 μm—most of the width of the central part of layer 1. In total they have a field of view of 0.6°.

Vertically, the field of view of the eye is extended by the dorsal and ventral extremities of the retina. Light reaching these regions must pass through the sides of the pit which, in longitudinal section, are straight beyond 10 μm from the optic axis and inclined at 30° to it. They produce a range of magnifications of 1.1–1.25, depending on the angle at which rays are incident. Magnification by the whole pit is therefore greatest on-axis, owing to the lens component, and decreases to a negligible amount for very off-axis light. Because off-axis magnification is different for different angles of incidence on the sides of the pit, off-axis focus will be blurred. This poorer image quality is reflected by the receptor mosaic off-axis in layers 1 and 2 where the rhabdoms are larger (~10 μm in diameter) and practically contiguous.

A jumping spider's field of view is extended horizontally by its lateral eyes which, in conjunction with the vertical extremities of the anterior median retinae, allow peripheral detection. Peripheral detection of an object initiates body and anterior median retinal movements that bring images of the object to lie in the centres of the retinae and maintain them there during fixation[6].

Land[3] suggested that the resolution of the anterior median eyes of two salticid species is probably limited by spherical aberration of their corneal lenses. Our re-examination of the lenses of *P. fimbriata* and several other salticids in a hanging drop and by interference microscopy shows that this defect is corrected by a graded refractive-index distribution in the lens, as in some nocturnal spiders[5,15,16]. Probably, then, the anterior median corneal lenses in salticids are diffraction limited. If this is true of the telephoto system of *P. fimbriata* as a whole, the maximum or cut-off spatial frequency passed by it is 760 rad^{-1} (refs 17–19). (The limiting aperture is a ring of pigment, 350 μm in diameter and 315 μm behind the corneal surface. The position of focus is taken as the distal ends of the receptors in layer 1. $\lambda = 520$ μm.) The highest spatial frequency that can be reconstructed by layer 1 with minimum receptor-row spacing 1.4 μm and distance 1,980 μm from the posterior nodal point of the telephoto system is $1{,}980/2.8 = 710$ rad^{-1}. Therefore, the receptor spacing in the centre of layer 1 seems to be well matched to the telephoto system. In the absence of the pit, the highest frequency reconstructable by the retina would be only 420 rad^{-1}, which is well below the cut-off frequency for the lens of 850 rad^{-1}.

A parallel to the pit of *P. fimbriata* is the deep convexiclivate fovea found in some vertebrates, notably falconiform birds[20]. It has been proposed that this fovea magnifies the retinal image[20,21] and acts as a focus indicator[22]. The latter is an implausible function for the pit in *P. fimbriata*, for as in other salticids[3], ophthalmoscopy shows that the eye does not accommodate. Aerodynamic constraints require the heads of birds to be small. Both a group of vertebrates and an invertebrate have therefore adopted the same strategy to improve visual acuity despite a restricted cephalic space.

We thank Robert Jackson for collecting *P. fimbriata* from Queensland, Fred Wanless (British Museum) for identifying them, and David Blest for his critical comments, for providing much anatomical information and for obtaining *Trite planiceps* in New Zealand with the help of Simon Pollard and Robert Jackson. Part of this report has been published elsewhere[23].

Received 28 July; accepted 20 October 1980.

1. Crane, J. *Zoologica* **34**, 159–214 (1949).
2. Drees, O. *Z. Tierpsychol.* **9**, 169–209 (1952).
3. Land, M. F. *J. exp. Biol.* **51**, 443–470 (1969).
4. Homann, H. *Z. vergl. Physiol.* **7**, 201–268 (1928).
5. Blest, A. D. & Land, M. F. *Proc. R. Soc.* **B196**, 197–222 (1977).
6. Land, M. F. *J. exp. Biol.* **51**, 471–493 (1969).
7. Longhurst, R. S. *Geometrical and Physical Optics* (Longman, London, 1973).
8. Blest, A. D., McIntyre, P. & Williams, D. S. (in preparation).
9. Blest, A. D., Hardie, R. C., McIntyre, P. & Williams, D. S. (in preparation).
10. De Voe, R. D. *J. gen. Physiol.* **66**, 193–207 (1975).
11. Yamashita, S. & Tateda, H. *J. comp. Physiol.* **105**, 29–41 (1976).
12. Forster, L. M. *N.Z. J. Zool.* **6**, 79–93 (1979).
13. Jackson, R. R. & Blest, A. D. (in preparation).
14. Snyder, A. W. *J. opt. Soc. Am.* **62**, 1267–1277 (1972).
15. Williams, D. S. *Z. Naturforsch.* **34c**, 463–469 (1979).
16. Blest, A. D., Williams, D. S. & Kao, L. *Cell Tissue Res.* **211**, 391–403 (1980).
17. Hopkins, H. H. *Proc. R. Soc.* **A231**, 91–103 (1955).
18. Born, M. & Wolf, E. *Principles of Optics*, 5th edn (Pergamon, Oxford, 1975).
19. Snyder, A. W. *J. comp. Physiol.* **116**, 161–182 (1977).
20. Walls, G. L. *The Vertebrate Eye* (Cranbrook Institute of Science, Bloomfield Hills, Michigan, 1942).
21. Snyder, A. W. & Miller, W. H. *Nature* **275**, 127–129 (1978).
22. Harkness, L. & Bennet-Clark, H. C. *Nature* **272**, 814–816 (1978).
23. Williams, D. S. & McIntyre, P. *Proc. Aust. physiol. pharmac. Soc.* 182P (1980).

Correlative genetic variation in natural populations of cats, mice and men

Stephen J. O'Brien,* Mitchell H. Gail† & David L. Levin†

* Laboratory of Viral Carcinogenesis, National Cancer Institute, National Institute of Health—Frederick Cancer Research Center, Frederick, Maryland 21701
† Biometry Branch, National Cancer Institute, National Institutes of Health, Bethesda, Maryland 20205

The study of the extent and basis of gene-enzyme variation has long been a principal concern of population genetics. Numerous surveys have indicated considerable amounts of genetic variation detectable in natural populations, with few exceptions[1–14]. The variances of average heterozygosities (H) between species and among populations within species are large, prompting Lewontin to emphasize the importance of large gene sample sizes[7] and Selander to encourage analysis of variation of